Mitigation of Cyanobacterial Harmful Algal Blooms by Electrochemical Ozonation: From Bench-scale Studies to Field Applications

Shasha Yang,[1,2] Luz Estefanny Quispe Cardenas,[1,2] Athkia Fariha,[1] Nada Shetewi,[3] Victor Melgarejo Cazares,[1,2] Nanyang Yang,[1] Lewis McCaffrey,[4] Nicole Wright,[4] Michael R. Twiss,[5] Siwen Wang,[1] Stefan J. Grimberg,[1] and Yang Yang[1]*

[1]Department of Civil and Environmental Engineering, Clarkson University, Potsdam, New York 13699, United States

[2]Institute for a Sustainable Environment, Clarkson University, Potsdam, New York 13699, United States

[3]Department of Chemical Engineering, The Cooper Union, New York, New York 10003, United States.

[4]New York State Department of Environmental Conservation, 625 Broadway, Albany, New York 12333, United States.

[5]Faculty of Science, Algoma University, Sault Ste. Marie, Ontario P6A 2G4, Canada.

ABSTRACT

Cyanobacterial harmful algal blooms (HABs) are an emerging threat to ecosystems, drinking water safety, and the recreational industry. As an environmental challenge intertwined with climate change and excessive nutrient discharge, HAB events occur more frequently and irregularly. This dilemma calls for fast-response treatment strategies. This study developed an electrochemical ozonation (ECO) process, which uses a Ni-Sb-SnO_2 anode to produce locally concentrated ozone (O_3) on electrodes to inactivate cyanobacteria and destroy microcystins within minutes. More importantly, the proof-of-concept was evolved into a full-scale boat-mounted completely mixed flow reactor for the treatment of HAB-impacted lake water at a treatment capacity of 544 m^3/d and energy consumption of < 1 Wh/L. Both lab-scale and full-scale investigations show that the byproducts (e.g., chlorate, bromate, trihalomethanes, and haloacetic acids) in the ECO-treated lake water were below the regulatory limits for drinking water. The whole effluent toxicity tests suggest that ECO treatment at 10 mA/cm^2 posed certain chronic toxicity to the model invertebrate (*Ceriodaphnia dubia*). However, the treatment at 7 mA/cm^2 (identified as the optimum condition) did not increase toxicity to model invertebrate and fish (*Pimephales promelas*) species. This study is a successful example of leveraging fundamental innovations in electrocatalysis to solve real-world problems.

Keywords: Harmful algal bloom, Microcystin, Ozone, Electrocatalysis, Tin oxide.

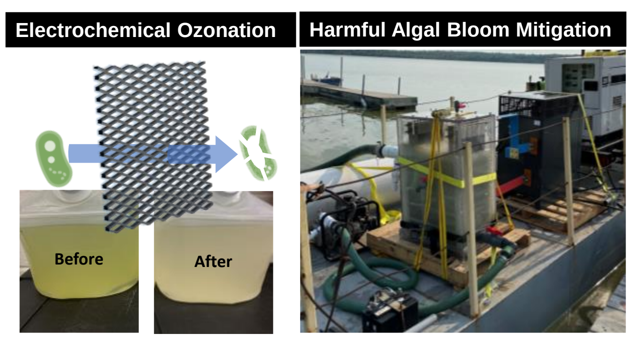

INTRODUCTION

Widespread cyanobacterial harmful algal blooms (HABs) have become an emerging threat to ecosystems, recreational use of lakes, and drinking water supplies. Due to increased nutrient discharge and global climate change, the occurrence of HABs is expected to be more frequent.[1,2] In the United States, the cyanobacterial HAB occurrence was 7 days per year per waterbody in 2017, and the frequency was projected to be 18-39 days per year per water body by 2090.[1] A recent study based on a 45-year record (1970 – 2015) revealed that the frequency of HABs occurring along the Chinese coast has increased by about 40% per decade.[3] The surge production of hepatotoxic, cytotoxic, and neurotoxic microcystins can be expected in the HAB events.[4]

Chemical oxidation (using chlorine, permanganate, H_2O_2, etc.)[5–7] and advanced oxidation processes (UV/H_2O_2 and UV/chlorine)[8] are promising for HAB mitigation at drinking water treatment works. However, they are less practical for on-site lake remediation due to the uncertain efficacy limited by hydrological conditions and concerns about the environmental impact of chemicals.

There is a critical need for *in situ* treatment technology that can proactively curb HABs at the early stage and precisely eliminate algae plumes in the impacted high-value areas (lake shores, public beaches, etc.). Since the bloom is usually concentrated at the top 0–1 m of the water column,[9,10] we envision that mobile devices with pump-and-treat functionality could realize the precise treatment of plume (instead of the whole water body) for maximum cost-effectiveness. Electrochemical oxidation (**EO**)-based technologies, with the advantages of small footprint, high efficiency, and chemical-free operation, could be the best fit. Previously, The EO treatment of algae and microcystins equipped with anodes made of boron-doped diamond,[11] metal oxide (RuO_2 and IrO_2),[12,13] and graphite[14] was investigated at the lab scale. We advanced the EO process by developing Ti_4O_7 filter anodes with pore sizes of 24−53 μm for the treatment of HAB-impacted lake water at both lab and full scales.[15] Similar to other reported anode materials, the Ti_4O_7 filter anodes oxidize chloride in lake water to chlorine to inactivate algae cells and oxidize cyanotoxins. The flow-through operation (by pumping water out of the filter anodes immersed in the plume) significantly promoted convective mass transfer and thereby achieved higher treatment performance than homogenous chlorination. Though the scaled-up demonstration at a capacity of 110 m^3/d was successful, two limitations were identified: (1) the chlorine yield, which is associated with treatment performance, depends on chloride concentrations in lake water. (2) The micropores of filter anode create large pressure drops ahead of the pump. Thus the treatment capacity is limited by the pump suction head, which is significantly smaller than the lift head. The pumps were also vulnerable to damage by cavitation.

This study aims to address these engineering challenges. First, the anode configuration was transformed from microporous cartridge filters to an array of mesh electrodes with rhombus 0.5×0.8 mm openings. Correspondingly, as will be discussed below, the treatment operation was changed to pumping water through the mesh electrode array in a boat-mount reactor. Second, the electrocatalysts were shifted from Ti_4O_7 to nickel-doped antimony tin oxide (**NATO**: Ni-Sb-SnO_2). The incentive is that NATO has unique reactivity toward ozone (**O_3**) evolution by water oxidation ($3H_2O \rightarrow O_3(g) + 6H^+ + 6e^-$, E^0=1.51 V_{RHE}).[16,17] Notably, NATO was deployed in organic degradation and disinfection.[18,19] However, its application in HAB mitigation was not explored. Because water is the only required precursor for ozone production, the shift of reactive species from free chlorine to O_3 enables the treatment performance to be independent of chloride concentration. In addition to process innovation, this study provides comprehensive evaluations of the environmental implications, covering process impacts on byproduct formation and effluent toxicity on an invertebrate and fish.

METHODS

Cyanobacteria Cultivation and Materials. Two cyanobacteria strains, *Synechococcus* sp. and *Microcystis aeruginosa* (UTEX Culture Collection of Algae), were incubated in a shaker incubator (Innova S44i, Eppendorf) with 10-30% photosynthetic light following our previous study.[15] The bench-scale tests involved mesh-type (0.5 × 0.8 mm rhombus openings) anode with either NATO or antimony tin oxide (ATO: Sb-SnO_2) coatings. The NATO and ATO anodes were prepared by dip-coating titanium mesh into sol-gel solutions of metal-citrate complexes, followed by calcination.[18] The NATO anode comprises NATO out-layer coating (1 mg/cm^2 projected area) and ATO base coating (1 mg/cm^2 projected area) on Ti mesh, while the ATO anode only contains the ATO base coating. The dual-layer design of the NATO anode bestows the electrode with superior durability and O_3 yield. Details were provided in our previous publication.[18] The full-scale electrode array contains 20 pieces of mesh NATO anode (50 × 50 cm; 0.5 × 0.8 mm rhombus openings) sandwiched by 21 pieces of perforated stainless steel sheet cathode (50 × 50 cm; round opening at Ø 3 mm) at an interspace of 0.5 cm. The full-scale mesh NATO anodes were manufactured by Square One Coating Systems following the same sol-gel coating + calcination procedure described above.

Testing Conditions. In bench-sale investigations, a mesh anode (NATO or ATO; 5 × 5 cm) was coupled with a stainless steel cathode (5 × 5 cm) at a distance of 0.5 cm and operated at current densities of 7 or 10 mA/cm^2. All tests were conducted in 95 mL phosphate buffer solution (**PBS**; pH = 7.7, conductivity = 329 µS/cm) or lake water collected from Lake Neatahwanta, NY. The synthetic water or lake water was spiked with cyanobacteria culture to reach an initial concentration of 100 µg/L as chlorophyll-a (Chl-a).

Analytical Approaches. Chl-a was measured by a fluorometer, and Microcystin LR (MC-LR) was quantified by liquid chromatography coupled with a quadrupole mass spectrometer (LC-MS/MS; Thermo Scientific, Vanquish-TSQ ALTIS). Details were described previously.[15] In the tests involving *Microcystis aeruginosa* (an MC-LR toxin-producing strain), MC-LR detected in the bulk solution was reported as extracellular MC-LR. Intracellular MC-LR was extracted by acetone after retaining cells by filtering the water sample through a polycarbonate membrane with a pore size of 0.2 µm.

Free chlorine was measured by a portable Hach DR900 colorimeter (HACH, CO) using a DPD (N,N-diethyl-p-phenylenediamine) reagent. Dissolved O_3 concentrations were determined by the indigo method on a NanoDrop OneC spectrophotometer (Thermo Fisher Scientific).[20] When measuring electrochemical O_3 evolution in the presence of chloride, the anodically generated free chlorine was masked by 1 M malonic acid.[18] Trihalomethanes (THMs) and haloacetic acids (HAAs) were measured by gas chromatography/mass spectrometry (GC/MS) following EPA Method 624.1. Inorganic anions were analyzed by ion chromatography (Thermo Dionex Integrion HPIC).[21] The whole effluent toxicity tests on *Pimephales promelas* and *Ceriodaphnia dubia* were independently conducted by AquaTOX Research, Inc., following EPA Methods 2000.0 and 2002.0 respectively (EPA-821-R-02-013).

RESULTS AND DISCUSSION

Electrode Characterization.

Figure 1a shows the cyclic voltammetric (CV) profiles of NATO and ATO. We adopted the Ni dopant level of 1 at.% (Ni/(Ni+Sb+Sn)) as optimized in previous studies.[16,22] The Ni doping shifts the CV hysteresis toward lower potentials. The rise of the current response at lower potentials can be attributed to the enhanced evolution of oxygen and O_3.[17] In the lake water treatment, the mesh electrodes were operated at current densities between 6-10 mA/cm^2 projected area, which leads to anodic potentials around 2.6-2.7 V_{RHE} (Figure 1a), surpassing the thermodynamic criteria for •OH radical evolution (•OH/H_2O: 2.7 V_{NHE}).[23]

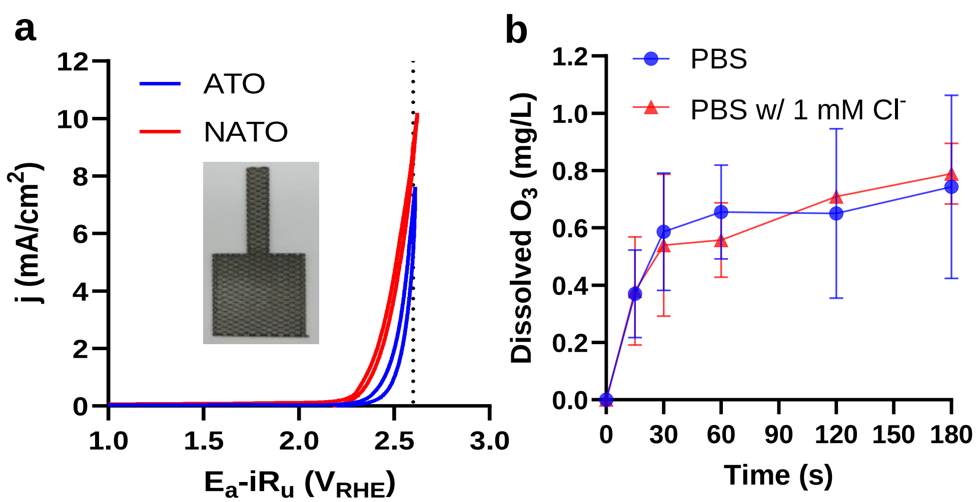

Figure 1. (a) Cyclic voltammetry of ATO and NATO anodes measured in 100 mM $NaClO_4$ electrolyte. (b) Dissolved O_3 produced by NATO at 10 mA/cm^2 in PBS electrolyte with and without 1 mM Cl^-. Data in Figure 1b are presented as the mean value of triplicate ± standard deviation.

Electrolysis using ATO could not generate O_3. In contrast, the NATO generated dissolved O_3 in PBS electrolyte in the presence or absence of Cl^- (Figure 1b). The evolution rate and current efficiency in PBS electrolyte at 10 mA/cm^2 are 0.0078 mmol/m^2/s and 4.5%, respectively. Chlorine evolution capability was tested in PBS electrolyte amended with 1 mM Cl^-, a typical Cl^- concentration found in lake waters treated in this study (Table S1). NATO and ATO demonstrated comparable chlorine evolution rates of 0.022 and 0.024 mmol/m^2/s, respectively, at 10 mA/cm^2 (Figure S1).

The electrochemical reactive surface area (ECSA) of the NATO mesh anode was measured by the double-layer capacitance method.[24] The capacitance is measured as 16.64 mF, corresponding to an ECSA of 443.6 cm^2 (Figure S2). The estimated ECSA is 8.9 times larger than the projected surface area (50 cm^2).

Bench-scale Investigation

The treatment performance of mesh-type ATO and NATO was evaluated based on the inactivation efficiency of *Synechococcus* and *Microcystis*, two strains of common cyanobacteria in algal blooms.[25,26] Because Chl-a cannot maintain its structural integrity and light-adsorbing properties after cell damage, it was used as an indicator to quantify the viable cell concentration as a generally accepted approach.[27–30] *Synechococcus* does not produce toxins. It was used in most bench-scale tests to study the kinetics of Chl-a degradation (i.e., cyanobacteria inactivation) without the interference of MC-LR. The optimized reaction conditions were then applied to treat electrolyte spiked with *Microcystis aeruginosa* culture with co-existing MC-LR.

The tests of inactivation of *Synechococcus* were first performed in PBS electrolyte at a current density of 10 mA/cm^2. Note that both ATO and NATO have sufficiently high anodic potentials of ~2.7 V_{RHE} to produce •OH (Figure 1a). If •OH is responsible for algae inactivation, ATO and NATO should exhibit similar performance. In contrast, it was found that ATO showed negligible reactivity in Chl-a removal, and NATO significantly outperformed ATO (Figure 2a). These results exclude the contribution of •OH-mediated oxidation and direct oxidation to cell inactivation, leaving electrochemically generated O_3 the only possible oxidant. The O_3 evolution on NATO involves the combination of surface-bound •OH with O_2 to form •HO_3, then O_3.[17,31] Therefore, the addition of 100 mM tert-butyl alcohol (TBA) to scavenge •OH halted the O_3 production (below detection limit), and thereby retarded Chl-a removal (Figure 2b).

In the presence of chloride, NATO could produce free chlorine and O_3. However, the addition of up to 3 mM Cl^- (a high record in lakes of the United States[32]) did not accelerate Chl-a removal (Figure 2b). Previously, we determined the pseudo-first-order rate constant of Chl-a in *Synechococcus* and free chlorine as 0.027 L/(mg min).[33] With the presence of 1 mM Cl^-, the time-average free chlorine concentrations produced by NATO at 10 mA/cm^2 within 120 s electrolysis should be ~7 mg/L (Figure S1). If free chlorine is responsible for Chl-a removal, the half-life of the reaction should be 220 s instead of the 48 s shown in Figure 2b.

The above investigations have excluded direct oxidation, •OH-mediated oxidation, and free chlorine-mediated oxidation as the dominant cyanobacteria inactivation (i.e., Chl-a removal) mechanisms, leaving electrochemical ozonation (**ECO**) the only pathway. The efficacy of ECO was compared with homogeneous ozonation (Figure 2c). The homogeneous ozonation at 1.5 mg/L O_3 achieved Chl-a removal kinetics similar to ECO. In contrast, ECO generated 0.48 mg/L

O_3 at 120 s, corresponding to a time-average [O_3] of 0.24 mg/L. ECO produced less bulk [O_3] (0.24 vs. 1.5 mg/L) to realize faster Chl-a removal kinetics than homogeneous ozonation. In other words, the cyanobacteria inactivation could be attributed to the locally concentrated O_3 produced at the anode surface, and the surficial O_3 concentration is equivalent to ~1.5 mg/L.

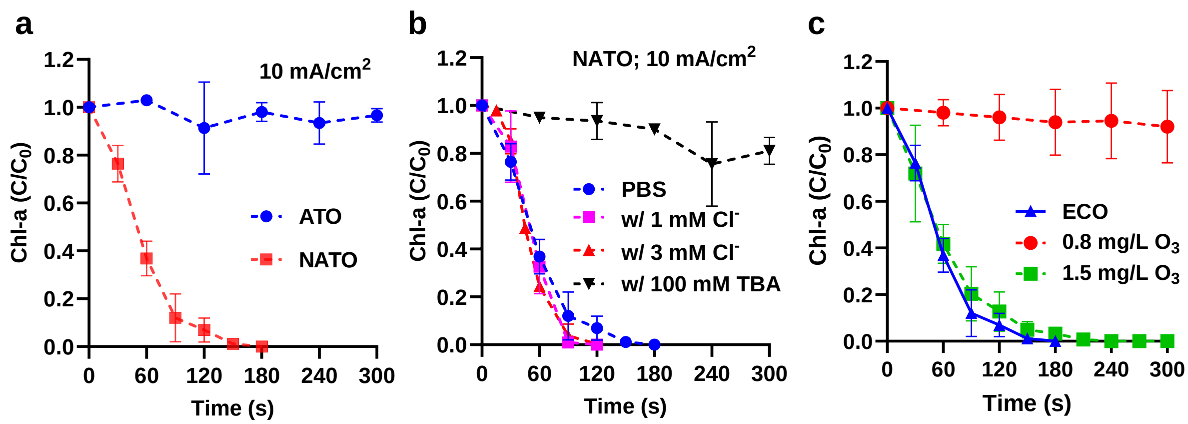

Figure 2. Inactivation of *Synechococcus* by electrolysis using (a) ATO and NATO anodes in PBS electrolyte and (b) NATO anode in different electrolytes. (c) Comparison of Chl-a destruction by ECO and homogeneous ozonation with various initial O_3 dosages (0.8 and 1.5 mg/L dissolved O_3). ECO tests were conducted in PBS at 10 mA/cm^2. Data are presented as the mean value of triplicate ± standard deviation.

After elucidating the reaction mechanism, the treatment tests were operated in more field-like scenarios. In most of the field tests, the ECO full-scale system was operated at 7 mA/cm^2 (see discussion below). At 7 mA/cm^2, ECO was effective in the removal of Chl-a in electrolytes with and without Cl^- (Figure S3). As shown in Figure 3a, the ECO process is equally efficient for the inactivation of *Microcystis aeruginosa* in PBS amended with 1 mM Cl^-. The treatment was further operated in Lake Neatahwanta water (collected before the HAB season and filtered to exclude background cyanobacteria and MC-LR) spiked with *Microcystis aeruginosa.* The Chl-a removal kinetics were slightly retarded by the water matrices, but the >90% removal efficiency can still be achieved after 180 s electrolysis. In contrast to *Synechococcus,* the *Microcystis aeruginosa* culture contains both intra- and extracellular MC-LR. The destruction of MC-LR consists of two parallel steps: (1) the lysed cells release intracellular MC-LR, which then become extracellular MC-LR in water, and (2) the destruction of existing and nascent extracellular MC-LR. The degradation of co-existing MC-LR in extra- and intra-cellular forms was investigated in PBS electrolyte amended with 1 mM Cl^- and lake water. In both media, extra-cellular MC-LR was subjected to faster degradation than intra-cellular MC-LR, as the degradation of the former required the destruction of cell structures (Figure 3b).

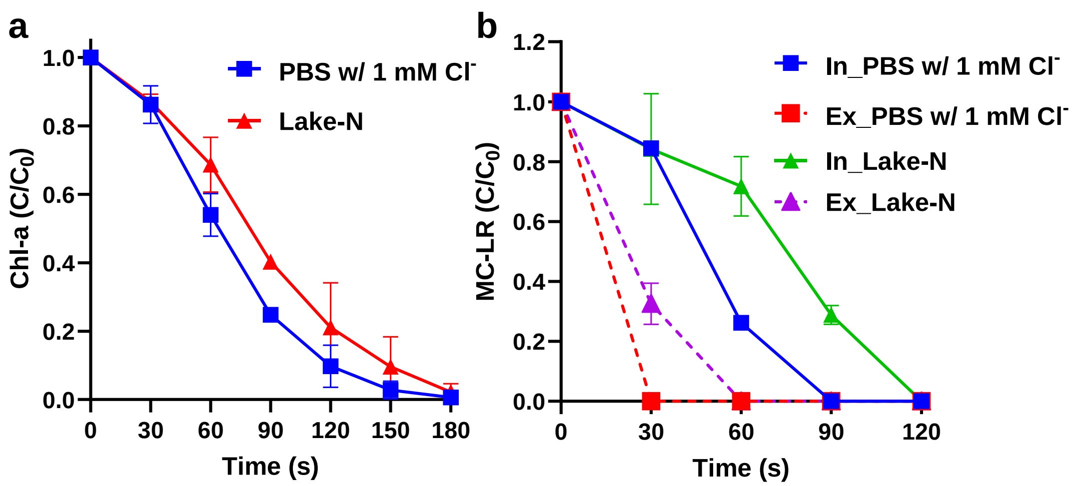

Figure 3. (a) Inactivation of *Microcystis aeruginosa* and (b) destruction of intracellular (In) and extracellular (Ex) MC-LR by electrolysis using NATO anode in PBS amended with 1 mM Cl^- and Lake Neatahwanta (Lake-N) water at 7 mA/cm^2. The initial Chl-a concentration is 100 µg/L. The initial concentrations of intracellular and extracellular MC-LR in PBS electrolyte are 1 and 3 µg/L , respectively. Data are presented as the mean value of triplicate ± standard deviation.

The bench-scale treatability study concluded that the ECO process is efficient for the removal of cyanobacteria and MC-LR at short, minute-level retention time. The remaining roadblock toward field development is understanding the environmental implications of the ECO technology. Given the fast Chl-a degradation kinetics, we hypothesize that significant cyanobacteria inactivation could be achieved before the yield of byproducts. Concern about the formation of inorganic byproducts was first addressed in the bench-scale study under field-like conditions. Other environmental aspects (organic byproducts and eco-toxicity) were investigated in the field application (see the following content). Chlorate (ClO_3^-) was identified as the product stemming from the electrochemical oxidation of Cl^-. Figure S4 shows the evolution of ClO_3^- in PBS electrolyte amended with 1 mM Cl^- and lake water containing ~1 mM Cl^- at 10 mA/cm^2. The results indicate that the evolution of ClO_3^- was suppressed in the lake water compared with electrolysis in PBS electrolytes, possibly due to the depletion of free chlorine by reacting with matrice components. As will be discussed below, the full-scale ECO reactor was operated at a Chl-a removal efficiency of ~40%, corresponding to a treatment duration of 60 s in batch mode. In this scenario, the [ClO_3^-] was below the detection limit (5 μg/L) and the World Health Organization (WHO) guideline of 0.7 mg/L.[34]

Bromate is a byproduct derived from the ozonation of bromide (Br^-).[35] We do not believe this is a concern in the lake water treatment in this study because Br^- was not detected in the lake water of two test sites (Table S1). To address the concern about the future applications in treating Br^- containing water, we investigated the formation BrO_3^- in the ECO treatment of PBS electrolyte containing 0.2 mg/L Br^-, a concentration reported in some surface water.[36] The results show that, throughout the 180 s ECO treatment process at 7 mA/cm^2, the dominant product is HOBr and BrO_3^- formation was not detected (Figure S5). This finding highlights the advantage of ECO over homogeneous ozonation as the former yields less bulk O_3 to form BrO_3^-.

The bench-scale investigation concludes that (1) ECO effectively removes cyanobacteria and cyanotoxins at short, minute-level retention times; (2) the reaction is built upon the locally concentrated O_3 produced at the NATO anode. The efficacy is independent of chloride concentration, which broadens the treatment scenarios in fresh waters.

Field Applications

A boat-mount ECO system was developed for the scaled-up treatment of HAB-impacted lake water (Figure 4a). The full-scale electrode array contains 20 pieces of mesh NATO anode (50 × 50 cm; 0.5 × 0.8 mm rhombus openings) sandwiched by 21 pieces of perforated stainless steel sheet cathode (50 × 50 cm; round opening at Ø 3 mm) at an interspace of 0.5 cm (Figure 4b). The polycarbonate reactor has a 190 L effective volume (excluding electrode array volume). Other on-board components include a custom-made DC power supply, generators, and a water pump. Algae plumes were captured by an intake pipe at an adjustable depth (0-1 m) underwater. An intake screen with a mesh opening size of 1 mm was installed on the intake port to prevent the entry of fish and other large aquatic life (Figure S6). Lake water was transferred from the pipe to the pump and pushed through the 190 L reactor at a flow rate of 378 L/min (i.e., treatment capacity of 544 m^3/d), corresponding to a hydraulic retention time of 30 s.

The electrode array has a total projected anode area of 10 m^2. Applying 600-1000 A total current on the electrode array resulted in current densities of 6-10 mA/cm^2 with a cell voltage ranging from 12-20 V. The electrode array was tightly packed in the reactor. In operation, water passing through the electrode mesh incurred efficient mass transfer. We have conducted preliminary tests in the field to show that the Chl-a concentrations in samples collected from the mid-height sampling port (representing bulk concentration) and outlet were the same (Figure S7). Therefore, the reactor can be considered a completely mixed-flow reactor (**CMFR**).

Based on the bench-scale batch reactions (data set of "PBS w/ 1 mM Cl^-" in Figures 2b and S3), the pseudo-first-order rate constants (k_{ECO}'s) at 7 and 10 mA/cm^2 are 0.026 and 0.061 s^{-1}, respectively. When transforming the reaction from batch to CMFR, the Chl-a removal efficiency can be estimated by

$$\text{Removal efficiency (\%)} = (1\text{-}C/C_0) \times 100\% = 1\text{-}1/(1+\tau k_{ECO}) \quad (1)$$

where C_0 and C are Chl-a concentrations in water entering and exiting the reactor, respectively. τ is the hydraulic retention time (30 s). Consequently, the removal efficiencies were projected as 44% and 64% for 7 and 10 mA/cm^2 operation, respectively, in CMFR mode.

The performance of the full-scale system was validated in the treatment of algal blooms that occurred in Lake Neatahwanta (43°18'30"N 76°26'14"W) and Oneida Lake (43°10'25"N 75°55'50"W) in New York state. Lake Neatahwanta was treated in the midst of an algal bloom with 105 μg/L Chl-a and 3 μg/L MC-LR, while tests on Oneida Lake happened in the early blooming stage with Chl-a concentration of 5.4 ug/L (Table S1). Each field deployment lasted for one day, with 9 to 12 pairs of influent and effluent samples taken. Tests in Oneida Lake were performed at current densities of 6-7 mA/cm^2, while those in Lake Neatahwanta were conducted at 7-10 mA/cm^2. As shown in Figure 4c, treatment operated at 7 and 10 mA/cm^2 achieved Chl-a removal efficiency of 39% and 62%, respectively, approaching the predicted values based on the CMFR model. More importantly, plotting removal efficiency data against specific energy consumption (Wh/L) shows that the field test performances align well with the bench-scale data set. The convergence of laboratory results and full-scale performance on Chl-a removal demonstrates the promising linear scalability of the ECO process in cyanobacteria inactivation using specific energy consumption as the key design parameter, given that the same anodes (i.e., NATO) are used.

Intracellular MC-LR was not found in the Lake Neatahwanta water samples. The treatment at 7 mA/cm^2 led to an effluent extracellular MC-LR concentration (i.e., MC-LR resides in lake water) of 0.41 μg/L (vs. C_0 = 3 μg/L), corresponding to a destruction efficiency of 86%. Note that it is challenging to study the extracellular MC-LR degradation kinetics due to the rapid degradation in ECO within a minute. Nonetheless, the 86% destruction of MC-LR when 40% Chl-a degradation was obtained in the full-scale CMFR reactor is comparable with the results observed in the lab-scale batch reactor (>95% destruction of MC-LR when ~40% Chl-a degradation was achieved, as shown in Figure 3).

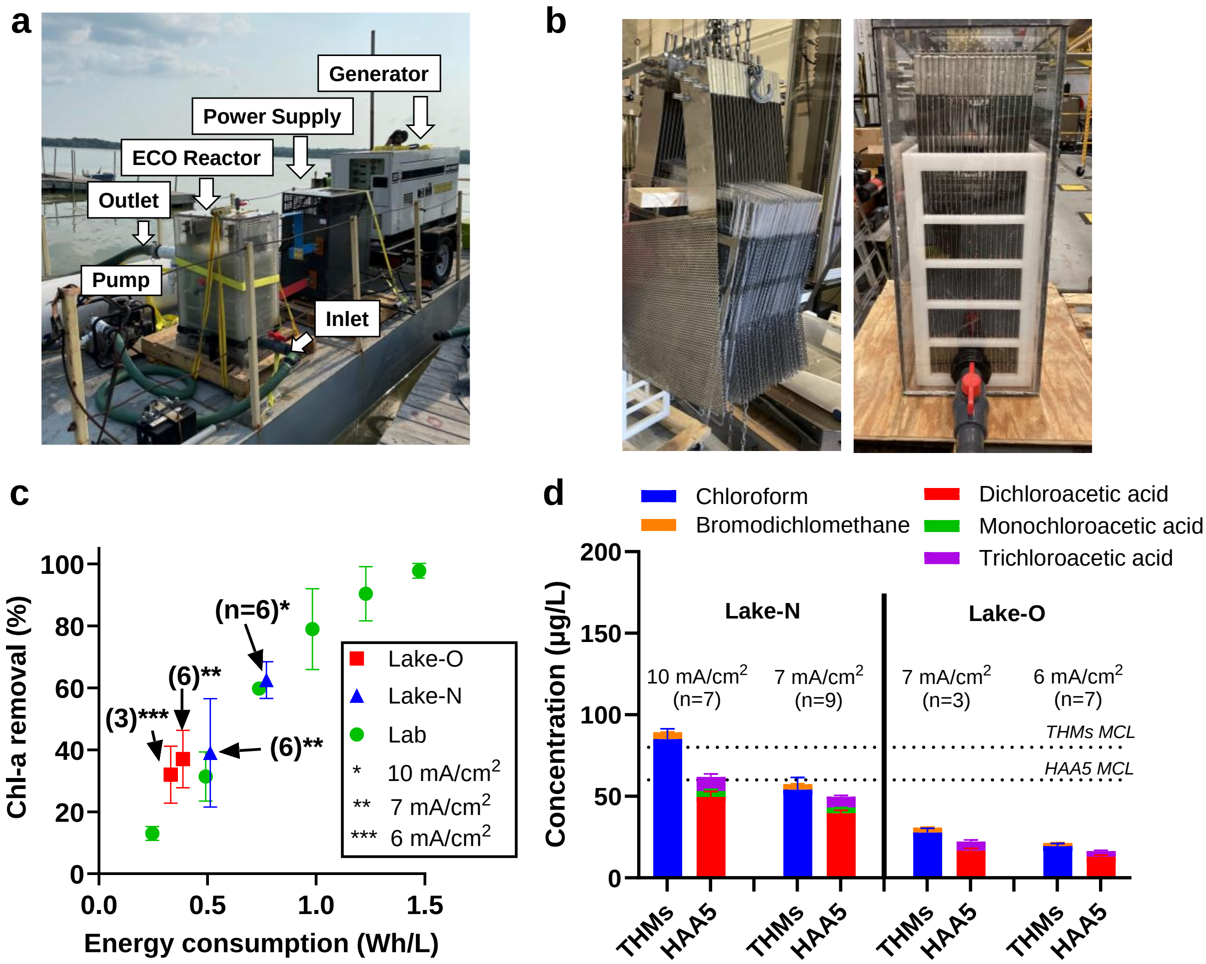

Figure 4. (a) Layout of the boat-mount ECO system. (b) Side view of ECO reactor with mesh electrodes installed. (c) Chl-a removal efficiencies benchmarked by energy consumption. Data were collected from lab-scale investigation and field tests performed in Lake Neatahwanta (Lake-N) and Oneida Lake Oneida (Lake-O). n is the number of pairs of inlet and outlet samples taken. (d) Trifluoromethanes (THMs) and five haloacetic acids (HAA5) in the treated Lake Neatahwanta effluent when the reactor was operated at 7 mA/cm^2. MCL is Maximum Contaminant Level regulated by U.S. EPA.

The current density of 7 mA/cm^2 (total current of 700 A and cell voltage of 14 V in treating Lake Neatahwanta) was identified as the optimum condition, balancing the significant algae removal, low byproduct formation, and insignificant toxicity (discussed below). It is important to note that the ~40% Chl-a removal at a short retention time of 30 s already incurred instant improvement in water clarity (Figure S8). Improvement in local water quality can be expected by the circulative treatment of water. The energy consumption of 0.5 Wh/L is also lower than the chlorine-based electrochemical HAB mitigation system (1.1 Wh/L) reported in our previous study.[33]

Environmental Implications.

The formation of halogenated byproducts, including trihalomethanes (THMs) and five haloacetate acids (HAA5), was investigated in the treatment of Lake Neatahwanta and Oneida Lake. THMs and HAA5 were not detected in the influent samples. In the effluent samples, chloroform and dichloroacetic acid were the dominant THMs and HAAs, respectively. For treatment operated at current densities of 6 and 7 mA/cm^2, the total concentrations of THMs and HAA5 were below the Maximum Contaminant Level (MCL) values regulated by the U.S. EPA (Figure 4d).

Whole effluent toxicity tests were conducted to evaluate whether the effluent from the ECO process would negatively impact the aquatic life in the receiving water. Samples of influent (INF) and treated effluent (EFF) were collected during the operation in Lake Neatahwanta (Table S2) and Oneida Lake (Table S3) at 6-10 mA/cm^2. In the toxicity tests, model freshwater invertebrate (*Ceriodaphnia dubia*) and fish (*Pimephales promelas*) species were exposed to INF samples, EFF samples, and lab control water (CON). Ten replicates were used for *Ceriodaphnia dubia,* and four replicates for *Pimephales promelas* for each INF, EFF, and CON exposure. Comparing the toxicity test results of samples obtained at 10 mA/cm^2 (Table S2), although *Ceriodaphnia dubia* survival was 100% at both 48 h (Acute) and 6-7 days (Chronic), reproduction is lower in EFF than INF, suggesting the treatment induced toxicity for the invertebrate species. Conversely, no effects were observed on the survival and growth of *Pimephales promelas*. The analysis of samples derived from operation at 6 and 7 mA/cm^2 show that there were no significant survival impacts at either 48 h (acute) or 6-7 days (chronic) for either the invertebrate or fish species, with survival rates of 100%. Similarly, there were no significant effects on the reproduction of invertebrates or growth of fish in EFF compared to INF. The whole effluent toxicity tests confirmed that the ECO process operated at 6 and 7 mA/cm^2 did not induce acute or chronic toxicity in the treated effluent, echoing our conclusion that 7 mA/cm^2 is the optimum current density.

CONCLUSIONS

This study developed an ECO process for the rapid inactivation of cyanobacteria and the destruction of MC-LR. The process used NATO anodes to generate locally concentrated O_3 as the major reactive species. Compared with homogeneous ozonation, the ECO process achieved the same degree of treatment but yielded lower bulk [O_3]. Note that a majority of electrochemical water treatment processes rely on the electrolysis of chloride to produce free chlorine as oxidants, and the treatment performance depends on the chloride concentration[37,38]. The shift of the dominant oxidant from chlorine to O_3 provides a new strategy for sustaining high treatment efficiency in freshwater with a limited chloride source and suppressing the formation of byproducts.

The significant merit of the engineering of this study is the scaled-up application of the ECO process to solve real-world problems. The performance of batch mode lab-scale reactor was replicated in a boat-mounted CMFR reactor using specific energy consumption as a benchmark. In addition to the successful demonstration of HAB mitigation, we also evaluated whole effluent toxicity to show that the ECO process operated at the optimized current density of 7 mA/cm^2 did not increase the effluent toxicity. This case study sets an example for the scaled-up application of electrified water treatment technology in environmental remediation.

ASSOCIATED CONTENT

Supporting Information

The Supporting Information is available free of charge at [Link].

The materials contain water composition, ECSA analysis, byproduct formation, and pictures of reactors.

ACKNOWLEDGMENTS

This research was supported by the New York State Center of Excellence in Healthy Water Solutions (C190175), New York State Department of Environmental Conservation (MOU# AM10700, ESF-PRJ-19-07) and Innovation Fund Manufacturing Grant (FuzeHub CON0002479). Opinions, results, findings and/or interpretations of data contained therein are the responsibility of the co-authors and do not necessarily represent the opinions, interpretations or policy of the State New York State. The New York State Department of Environmental Conservation funding does not imply endorsement of commercial products, currently or in the future. We thank Scott Hodge and Jacob Weller of the Clarkson University Machine Shop for assembling and modifying the boat-mount ECO system. We thank Clarkson University graduate students Bryan Dwyer and Philip Hekeler for their assistance in field operations.

REFERENCES

(1) Chapra, S. C.; Boehlert, B.; Fant, C.; Bierman, V. J.; Henderson, J.; Mills, D.; Mas, D. M. L.; Rennels, L.; Jantarasami, L.; Martinich, J.; Strzepek, K. M.; Paerl, H. W. Climate Change Impacts on Harmful Algal Blooms in U.S. Freshwaters: A Screening-Level Assessment. *Environ. Sci. Technol.* **2017**, *51* (16), 8933–8943. https://doi.org/10.1021/acs.est.7b01498.

(2) Paerl, H. W.; Scott, J. T. Throwing Fuel on the Fire: Synergistic Effects of Excessive Nitrogen Inputs and Global Warming on Harmful Algal Blooms. *Environ. Sci. Technol.* **2010**, *44* (20), 7756–7758. https://doi.org/10.1021/es102665e.

(3) Xiao, X.; Agustí, S.; Pan, Y.; Yu, Y.; Li, K.; Wu, J.; Duarte, C. M. Warming Amplifies the Frequency of Harmful Algal Blooms with Eutrophication in Chinese Coastal Waters. *Environ. Sci. Technol.* **2019**, *53* (22), 13031–13041. https://doi.org/10.1021/acs.est.9b03726.

(4) Dong, H.; Aziz, Md. T.; Richardson, S. D. Transformation of Algal Toxins during the Oxidation/Disinfection Processes of Drinking Water: From Structure to Toxicity. *Environ. Sci. Technol.* **2023**. https://doi.org/10.1021/acs.est.3c01912.

(5) Xie, P.; Ma, J.; Fang, J.; Guan, Y.; Yue, S.; Li, X.; Chen, L. Comparison of Permanganate Preoxidation and Preozonation on Algae Containing Water: Cell Integrity, Characteristics, and Chlorinated Disinfection Byproduct Formation. *Environ. Sci. Technol.* **2013**, *47* (24), 14051–14061. https://doi.org/10.1021/es4027024.

(6) Zamyadi, A.; Fan, Y.; Daly, R. I.; Prévost, M. Chlorination of Microcystis Aeruginosa: Toxin Release and Oxidation, Cellular Chlorine Demand and Disinfection by-Products Formation. *Water Res.* **2013**, *47* (3), 1080–1090. https://doi.org/10.1016/j.watres.2012.11.031.

(7) Spoof, L.; Jaakkola, S.; Važić, T.; Häggqvist, K.; Kirkkala, T.; Ventelä, A.-M.; Kirkkala, T.; Svirčev, Z.; Meriluoto, J. Elimination of Cyanobacteria and Microcystins in Irrigation Water—Effects of Hydrogen Peroxide Treatment. *Environ. Sci. Pollut. Res.* **2020**, *27* (8), 8638–8652. https://doi.org/10.1007/s11356-019-07476-x.

(8) Yu, B.; Zhang, Y.; Wu, H.; Yan, W.; Meng, Y.; Hu, C.; Liu, Z.; Ding, J.; Zhang, H. Advanced Oxidation Processes for Synchronizing Harmful Microcystis Blooms Control with Algal Metabolites Removal: From the Laboratory to Practical Applications. *Sci. Total Environ.* **2024**, *906*, 167650. https://doi.org/10.1016/j.scitotenv.2023.167650.

(9) Kutser, T. Quantitative Detection of Chlorophyll in Cyanobacterial Blooms by Satellite Remote Sensing. *Limnol. Oceanogr.* **2004**, *49* (6), 2179–2189. https://doi.org/10.4319/lo.2004.49.6.2179.

(10) Moore, T. S.; Churnside, J. H.; Sullivan, J. M.; Twardowski, M. S.; Nayak, A. R.; McFarland, M. N.; Stockley, N. D.; Gould, R. W.; Johengen, T. H.; Ruberg, S. A. Vertical Distributions of Blooming Cyanobacteria Populations in a Freshwater Lake from LIDAR Observations. *Remote Sens. Environ.* **2019**, *225*, 347–367. https://doi.org/10.1016/j.rse.2019.02.025.

(11) Liao, W.; Murugananthan, M.; Zhang, Y. Electrochemical Degradation and Mechanistic Analysis of Microcystin-LR at Boron-Doped Diamond Electrode. *Chem. Eng. J.* **2014**, *243*, 117–126. https://doi.org/10.1016/j.cej.2013.12.091.

(12) Liang, W.; Qu, J.; Chen, L.; Liu, H.; Lei, P. Inactivation of Microcystis Aeruginosa by Continuous Electrochemical Cycling Process in Tube Using Ti/RuO2 Electrodes. *Environ. Sci. Technol.* **2005**, *39* (12), 4633–4639. https://doi.org/10.1021/es048382m.

(13) Zhou, Y.; Peng, H.; Jiang, L.; Wang, X.; Tang, Y.; Xiao, L. Control of Cyanobacterial Bloom and Purification of Bloom-Laden Water by Sequential Electro-Oxidation and Electro-Oxidation-Coagulation. *J. Hazard. Mater.* **2024**, *462*, 132729. https://doi.org/10.1016/j.jhazmat.2023.132729.

(14) Huang, C.; Huang, W.; Xiong, J.; Wang, S. Mechanism and Excellent Performance of Graphite Felt as Anodes in Electrochemical System for Microcystis Aeruginosa and Microcystin-LR Removal with No pH Limitation nor Chemical Addition. *Sep. Purif. Technol.* **2021**, *277*, 119502. https://doi.org/10.1016/j.seppur.2021.119502.

(15) Yang, S.; Twiss, M. R.; Fernando, S.; Grimberg, S. J.; Yang, Y. Mitigation of Cyanobacterial Harmful Algal Blooms (cHABs) and Cyanotoxins by Electrochemical Oxidation: From a Bench-Scale Study to Field Application. *ACS EST Eng.* **2022**. https://doi.org/10.1021/acsestengg.1c00344.
(16) Christensen, P. A.; Zakaria, K.; Christensen, H.; Yonar, T. The Effect of Ni and Sb Oxide Precursors, and of Ni Composition, Synthesis Conditions and Operating Parameters on the Activity, Selectivity and Durability of Sb-Doped SnO2 Anodes Modified with Ni. *J. Electrochem. Soc.* **2013**, *160* (8), H405. https://doi.org/10.1149/2.023308jes.
(17) Christensen, P. A.; Attidekou, P. S.; Egdell, R. G.; Maneelok, S.; Manning, D. A. C.; Palgrave, R. Identification of the Mechanism of Electrocatalytic Ozone Generation on Ni/Sb-SnO2. *J. Phys. Chem. C* **2017**, *121* (2), 1188–1199. https://doi.org/10.1021/acs.jpcc.6b10521.
(18) Zhang, Y.; Yang, Y.; Yang, S.; Quispe-Cardenas, E.; Hoffmann, M. R. Application of Heterojunction Ni–Sb–SnO2 Anodes for Electrochemical Water Treatment. *ACS EST Eng.* **2021**, *1* (8), 1236–1245. https://doi.org/10.1021/acsestengg.1c00122.
(19) Yang, S. Y.; Kim, D.; Park, H. Shift of the Reactive Species in the Sb–SnO2-Electrocatalyzed Inactivation of E. Coli and Degradation of Phenol: Effects of Nickel Doping and Electrolytes. *Environ. Sci. Technol.* **2014**, *48* (5), 2877–2884. https://doi.org/10.1021/es404688z.
(20) Bader, H.; Hoigné, J. Determination of Ozone in Water by the Indigo Method. *Water Res.* **1981**, *15* (4), 449–456. https://doi.org/10.1016/0043-1354(81)90054-3.
(21) Yang, S.; Fernando, S.; Holsen, T. M.; Yang, Y. Inhibition of Perchlorate Formation during the Electrochemical Oxidation of Perfluoroalkyl Acid in Groundwater. *Environ. Sci. Technol. Lett.* **2019**, *6* (12), 775–780. https://doi.org/10.1021/acs.estlett.9b00653.
(22) Yang, S. Y.; Choo, Y. S.; Kim, S.; Lim, S. K.; Lee, J.; Park, H. Boosting the Electrocatalytic Activities of SnO2 Electrodes for Remediation of Aqueous Pollutants by Doping with Various Metals. *Appl. Catal. B Environ.* **2012**, *111–112*, 317–325. https://doi.org/10.1016/j.apcatb.2011.10.014.
(23) Yang, Y. Recent Advances in the Electrochemical Oxidation Water Treatment: Spotlight on Byproduct Control. *Front. Environ. Sci. Eng.* **2020**, *14* (5), 85. https://doi.org/10.1007/s11783-020-1264-7.
(24) McCrory, C. C. L.; Jung, S.; Peters, J. C.; Jaramillo, T. F. Benchmarking Heterogeneous Electrocatalysts for the Oxygen Evolution Reaction. *J. Am. Chem. Soc.* **2013**, *135* (45), 16977–16987. https://doi.org/10.1021/ja407115p.
(25) Li, J.; Chen, Z.; Jing, Z.; Zhou, L.; Li, G.; Ke, Z.; Jiang, X.; Liu, J.; Liu, H.; Tan, Y. Synechococcus Bloom in the Pearl River Estuary and Adjacent Coastal Area–With Special Focus on Flooding during Wet Seasons. *Sci. Total Environ.* **2019**, *692*, 769–783. https://doi.org/10.1016/j.scitotenv.2019.07.088.
(26) D'ors, A.; Bartolomé, M. C.; Sánchez-Fortún, S. Toxic Risk Associated with Sporadic Occurrences of Microcystis Aeruginosa Blooms from Tidal Rivers in Marine and Estuarine Ecosystems and Its Impact on Artemia Franciscana Nauplii Populations. *Chemosphere* **2013**, *90* (7), 2187–2192. https://doi.org/10.1016/j.chemosphere.2012.11.029.
(27) Schulze, K.; López, D. A.; Tillich, U. M.; Frohme, M. A Simple Viability Analysis for Unicellular Cyanobacteria Using a New Autofluorescence Assay, Automated Microscopy, and ImageJ. *BMC Biotechnol.* **2011**, *11* (1), 118. https://doi.org/10.1186/1472-6750-11-118.
(28) Sun, F.; Pei, H.-Y.; Hu, W.-R.; Song, M.-M. A Multi-Technique Approach for the Quantification of Microcystis Aeruginosa FACHB-905 Biomass during High Algae-Laden Periods. *Environ. Technol.* **2012**, *33* (15), 1773–1779. https://doi.org/10.1080/09593330.2011.644868.
(29) Hazeem, L. J.; Kuku, G.; Dewailly, E.; Slomianny, C.; Barras, A.; Hamdi, A.; Boukherroub, R.; Culha, M.; Bououdina, M. Toxicity Effect of Silver Nanoparticles on Photosynthetic Pigment Content, Growth, ROS Production and Ultrastructural Changes of Microalgae Chlorella Vulgaris. *Nanomaterials* **2019**, *9* (7), 914. https://doi.org/10.3390/nano9070914.

(30) Song, Y.; Li, Z.; Feng, A.; Zhang, J.; Liu, Z.; Li, D. Electrokinetic Detection and Separation of Living Algae in a Microfluidic Chip: Implication for Ship's Ballast Water Analysis. *Environ. Sci. Pollut. Res.* **2021**, *28* (18), 22853–22863. https://doi.org/10.1007/s11356-020-12315-5.
(31) Wang, Y.-H.; Chen, Q.-Y. Anodic Materials for Electrocatalytic Ozone Generation. *Int. J. Electrochem.* **2013**, *2013*, 1–7. https://doi.org/10.1155/2013/128248.
(32) Dugan, H. A.; Bartlett, S. L.; Burke, S. M.; Doubek, J. P.; Krivak-Tetley, F. E.; Skaff, N. K.; Summers, J. C.; Farrell, K. J.; McCullough, I. M.; Morales-Williams, A. M.; Roberts, D. C.; Ouyang, Z.; Scordo, F.; Hanson, P. C.; Weathers, K. C. Salting Our Freshwater Lakes. *Proc. Natl. Acad. Sci.* **2017**, *114* (17), 4453–4458. https://doi.org/10.1073/pnas.1620211114.
(33) Yang, S.; Twiss, M. R.; Fernando, S.; Grimberg, S. J.; Yang, Y. Mitigation of Cyanobacterial Harmful Algal Blooms (cHABs) and Cyanotoxins by Electrochemical Oxidation: From a Bench-Scale Study to Field Application. *ACS EST Eng.* **2022**, *2* (7), 1160–1168. https://doi.org/10.1021/acsestengg.1c00344.
(34) World Health Organization. Chlorite and Chlorate in Drinkingwater, WHO Guidelines for Drinkingwater Quality; WHO/SDE/WSH/05.08/86, 2005.
(35) Legube, B.; Parinet, B.; Gelinet, K.; Berne, F.; Croue, J.-P. Modeling of Bromate Formation by Ozonation of Surface Waters in Drinking Water Treatment. *Water Res.* **2004**, *38* (8), 2185–2195. https://doi.org/10.1016/j.watres.2004.01.028.
(36) *Bromide in Surface Waters*. Capps Lab at UGA. http://cappslab.ecology.uga.edu/additional-info/bromide-in-surface-water/ (accessed 2023-10-13).
(37) Yang, Y.; Shin, J.; Jasper, J. T.; Hoffmann, M. R. Multilayer Heterojunction Anodes for Saline Wastewater Treatment: Design Strategies and Reactive Species Generation Mechanisms. *Environ. Sci. Technol.* **2016**, *50* (16), 8780–8787. https://doi.org/10.1021/acs.est.6b00688.
(38) Cho, K.; Qu, Y.; Kwon, D.; Zhang, H.; Cid, C. A.; Aryanfar, A.; Hoffmann, M. R. Effects of Anodic Potential and Chloride Ion on Overall Reactivity in Electrochemical Reactors Designed for Solar-Powered Wastewater Treatment. *Environ. Sci. Technol.* **2014**, *48* (4), 2377–2384. https://doi.org/10.1021/es404137u.